

CHAPTER 171

The Analysis and Role of Bars on the Protection of a Beach System Gold Coast, Queensland, Australia

B. Boczar-Karakiewicz¹ and L.A. Jackson²

Abstract

Gold Coast beach profile changes have been analysed using a dynamical model describing wave-bed interactions. The model explains the formation and dynamics of prominent longshore bars which are characteristic features of the studied nearshore. Model predictions are compared with field observations and measurements in several locations. Obtained results justify protection measures (eg. nourishment of offshore bars) applied in the study area by the Gold Coast City Council.

1. Introduction

According to observations over a period of the last 100 years, the beach system in the Gold Coast (Fig.1) area is extremely dynamic. At times of severe storm and cyclones events, the beaches are exposed to

high energy waves up to 8.5 m with corresponding wave periods of 14.0 secs. The amplitudes of highest waves observed in this region over to 12.0 m and the largest wave periods are of 17-18 secs (McGrath and Robinson 1973, Gold Coast City Council 1990).

In those conditions, the beaches are eroded but subsequently restored under mild weather conditions and swell waves. After the worst recorded erosion in 1967, the recovery of the

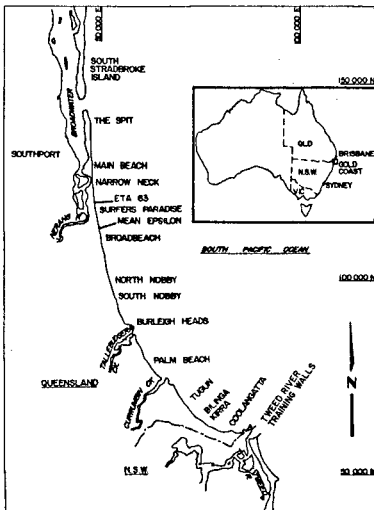


Figure 1. Location map

¹Professor, INRS-Océanologie, Rimouski (Québec) Canada, G5L 3A1

²Engineer, Gold Coast City Council, QLD 4217, Australia

upper beach took a period of some 18 months. With a frequency of major storm and cyclone events lower than 1/18 month, the beach system may recover under conditions that a natural buffer zone comprising the dunes is conserved, and that the sediment supply from the local Tweed River compensates losses of sediment due to the wave-induced longshore transport (Jackson, Smith and Piggot 1988). However, the conservation of a sufficiently large natural dune system has been difficult given the rapid expansion of the recreational usage of the Gold Coast area (Smith and Jackson 1990). Additionally, the construction and subsequent extension of the training walls of the Tweed River (1910 and 1964, respectively) have significantly modified the local sediment supply. The extension of the walls caused an approximated deficit of sediment of some 250,000 m³/yr. Therefore, in recent years quite severe effects of erosion were observed mainly in the southern part of the Gold Coast propelling gradually downdrift to central beaches.

To date some 9 M m³ of beach nourishment has been carried out but protection of the beach and foreshore development requires more beach nourishment to compensate intrusion into the active beach zone by past developments (Chapman 1980, Smith and Jackson 1990). Nourishment has been placed onshore, nearshore and a combination of both. The cost and efficiency of nourishment varies considerably with the location of placement. As nearshore nourishment is generally considerably less expensive in the Gold Coast case, research has been carried out on the behaviour of natural and artificial (nourished) nearshore bars.

To better understand the natural beach system and the effect of natural and artificial bars on the protection of the upper beach, a model has been developed. An analysis of beach equilibrium is presented and based on observations and mathematical modelling of large scale sand bars which are prominent features of the Gold Coast nearshore. Aerial photography shows evidence of offshore sand bars in the entire nearshore of the Gold Coast area. The geometry of bars, their appearance and stability varies in different parts of the coast. Generally they are strongly related to the incidence of predominant storm waves and swell. Typically, the outer shore-parallel bar lies in a water depth of 6-10 m and at distances of 400-500 m from the mean position of the shoreline.

The Gold Coast beach system is extremely mobile with changes occurring in several very different time scales: incident wave trains are changing during normal weather conditions in several tens of hours, the weather over a few days, the climate over years, sediment supply over decades and the shape of the seabed in days to several months.

Observations and measurements show, however, that the complex beach system periodically reaches some kind of dynamical equilibrium which in turn is controlled only by two main factors. These factors are the incident waves and the shape of the underlying seabed from its deepwater end (extending to some 20-25 m of water depth) up to the visible beach (Smith and Jackson 1990).

The incident wave and seabed parameters are the only free parameters in the dynamical model applied in the presented analysis. Model predictions have been compared with observations and resulting conclusions justify the use of nearshore nourishment as a protection measure applied in the study area by the Gold Coast City Council.

2. The model

The model has four constituent processes describing wave-bed interactions, namely (1) the hydrodynamics of the main water body, (2) the near-bed boundary-layer flow, (3) the sediment transport, and (4) the evolution of the bed topography. These four modules are linked together and the resulting model is discretized for numerical integration. The integration procedure consists of a two-step time loop. In the first step, the fluid flow and the sediment flux are calculated over a bed configuration which is instantaneously fixed. In the second step, the temporal evolution of the seabed is calculated while keeping all variables describing the fluid and sediment flow constant. This two-step approximation is justified both on mathematical grounds, and by observations in the laboratory and natural coastal environments which indicates significant changes in bed topography are only observed over a period of many thousands of wave periods. A time-scale is quite long when compared to rapid changes in the fluid flow that can occur during one wave period (Boczar-Karakiewicz *et al.* 1987, Boczar-Karakiewicz and Davidson-Arnott 1987).

The first model constituent describes surface-wave motion in a typical nearshore setting in which the wavelength λ of a peak-period storm wave is large, compared with local water depth h . Following Keller (1988), the recent surface wave description has been derived directly from Euler equations and continuity for a fluid flow bounded by a free surface at $\bar{z} = \zeta(\bar{x}, \bar{t})$, and by a fixed bed at $\bar{z} = -\bar{h}(\bar{x})$. Application of Keller's approach allows us to solve the earlier defined problem of wave propagation in three spatial dimensions in a curvilinear coordinate system (x, z) , where x , is the path of the wave ray (Boczar-Karakiewicz *et al.* 1990).

At the present stage of modelling, it is assumed that the incident waves and the nearshore bathymetry do not vary appreciably in the longshore direction so that both the wave and bed motion are two-dimensional as indicated in Figure 2.

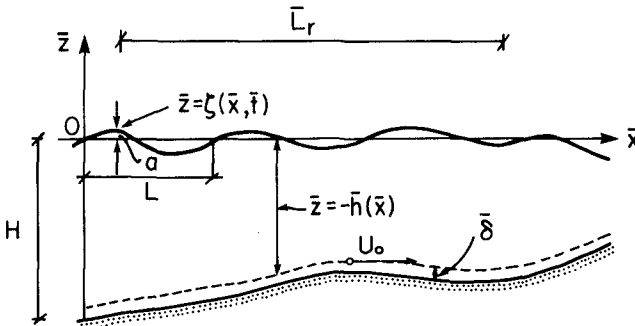


Figure 2. Notation scheme

In this idealized version of the bed-fluid system, it is assumed that the incident wave propagates shoreward from the deep water end of the nearshore and that the incoming wave train is of constant amplitude and frequency. The horizontal coordinate, in Figure 2, is $\bar{x} = 0$ at the deep end of the nearshore where $\bar{z} = -H$, \bar{z} is the vertical coordinate with $\bar{z} = 0$ at the undisturbed, free water surface. The surface wave is assumed to be progressive in the whole spatial domain and the free surface elevation ζ is expanded into a power series and modally decomposed,

$$\zeta = \zeta(x, X, t) = \sum_{j=1}^2 a_j(X) \exp(ik_j x - i\omega_j t) + c.c., \quad (1)$$

In equation (1), X is an independent, horizontal variable defined by $X = B \cdot x$. The small parameter β ($\beta \leq 0.1$) is evaluated from incident water depth H , and wave length λ , thus $\beta = H/\lambda$. The notation c.c. stands for the complex conjugate of the quantity just preceding it, so in this case,

$$c.c. = \sum_{j=1}^2 a_j^*(X) \exp(i\omega_j t - ik_j x).$$

In equation (1), ω_1 is the frequency of the postulated incoming wave train and $\omega_2 = 2\omega_1$ is its second harmonic, k_1 and k_2 are wave numbers associated with ω_1 and ω_2 , respectively. The complex, first order amplitudes a_1 and a_2 are taken to vary on the scale of wave lengths, and therefore, are dependent only on the variable X . The symbol a_j^* denotes the complex conjugate of a_j . In equation (1), dimensional variables have been nondimensionalized and scaled according to the scheme,

$$(h, x, z) = \frac{1}{H} \bar{h}, \bar{x}, \bar{z}, t = (g/H)^{1/2} \bar{t}, \zeta = \frac{1}{\alpha H} \bar{\zeta}, \quad (2)$$

where H denotes a characteristic water depth (e.g. depth at the deep water end), g is the magnitude of acceleration due to gravity, and $\alpha = a/H$, where a denotes the wave amplitude. A similar representation to equation (1) is postulated for the velocity potential ϕ . Assuming the principal features of the bottom variation to be gradual, it may also be taken that h is a function $h(X)$ of the variable X , only.

Requirements that ζ and ϕ are to satisfy Euler equations and continuity, in conjunction with the above hypotheses yield the linear dispersion relation from which k_1 and k_2 are determined,

$$k_j \tanh k_j h = \omega_j^2, \quad j = 1, 2. \quad (3)$$

Solvability conditions for the second order solutions provide a coupled pair of nonlinear ordinary differential equations for the complex amplitudes a_1 and a_1^* ,

$$\frac{da_1}{dx} = - \frac{1}{2C_1} \frac{dC_1}{dx} a_1 - \frac{1}{2} i \frac{\alpha}{\beta} a_1^* a_2 \exp(-i \frac{\Delta k}{\beta} x) \frac{B_1}{C_1} \tag{4}$$

$$\frac{da_2}{dx} = - \frac{1}{2C_2} \frac{dC_2}{dx} a_2 - \frac{1}{2} i \frac{\alpha}{\beta} a_2^2 \exp(i \frac{\Delta k}{\beta} x) \frac{B_2}{C_2}$$

where functional coefficients B_j ($j = 1,2$) depend on ω_j , k_j and X . The symbols C_j and dC_j/dX in (4) denote the group velocity and its spatial derivative given in the present approximation by following expressions,

$$C_j = \frac{1}{2} \frac{1}{\omega_j k_j} [\omega_j^2 - h(\omega_j^4 - k_j^2)]; \quad j = 1, 2, \tag{5}$$

$$\frac{dC_j}{dx} = \frac{k_j^2 - \omega_j^2}{k_j} \frac{\omega_j (h\omega_j^2 - 1)}{\omega_j^2 (h\omega_j^2 - 1) - hk_j^2} \cdot \frac{dh}{dx}, \quad j = 1, 2,$$

and $\Delta k = 2k_1 - k_2$ denotes the difference of wave numbers of the two modal wave components in equation (1).

As shown by Keller (1988), equations (4) are coupled transport equations. The linear dispersion relation, equation (3) and the transport equations (4) constitute the first component of the model. These equations, when supplemented with boundary conditions for α , ω_1 , a_1 and a_1^* at $X = 0$, provide an approximate description of the evolution of the waveform ζ and associated velocity field over a given bed configuration h .

The derivation of the second and third model constituents in which the boundary layer flow and resulting sediment flux are evaluated have been presented in earlier work (Boczar-Karakiewicz and Bona 1986, Chapalain and Boczar-Karakiewicz 1989, Boczar-Karakiewicz *et al.* 1987).

The fourth model constituent relates through continuity the differential of the sediment flux $\partial Q/\partial X$ to the desired temporal evolution of the seabed topography h , thus,

$$\frac{\partial h}{\partial \tau} = \chi \frac{\partial Q}{\partial X} \tag{6}$$

where τ is the time scale of bed deformation and χ denotes the threshold constant. Equation (6) has to be supplemented by sediment parameters (grain diameter, fall velocity, etc.) required in the second, third and fourth model constituents.

Eventually, the coupled system of equations (4),(5) and (6) supplemented by boundary conditions specifying the incident wave parameters (α , ω_1 , a_1 , a_1^*), the initial bed topography h' at $\tau = 0$, and

sediment characteristics, constitutes the dynamic description for wave-bottom interactions.

Results of a typical numerical experiment with a set of incident and initial data for waves of $T = 17$ s and a uniform sloping bed ($\tan \phi = 0.0125$) are presented in Figures 4a-d. At the chosen incident water depth $H = 18$ m the incident wave is assumed to "feel" the presence of a shallow seabed ($\beta = H/\lambda = 0.1$). The incident wave parameter $\alpha = a/H = 0.1$. Selected wave and bed data characterize an extreme cyclonic event in the central region of the Gold Coast area (Broadbeach, see Figure 1 for location).

The instantaneous wave profile ζ over the final bed profile (at $t = 6 \Delta\tau$) is shown in Figure 3a. The harmonic amplitudes $|a_1|$ and $|a_2|$ of the two modal components of the interface ζ are presented in Figure 3b and the relative phases between a_1 and a_2 , $\psi = k_1 - 2k_2 + \arg a_2 - 2 \arg a_1$, are shown in Figure 3c. The initial and final state of the bed topography is shown in Figure 3d (at $t = 0$ and $t = 6 \Delta\tau$, respectively) and $\Delta\tau$ denotes the time step in this experiment.

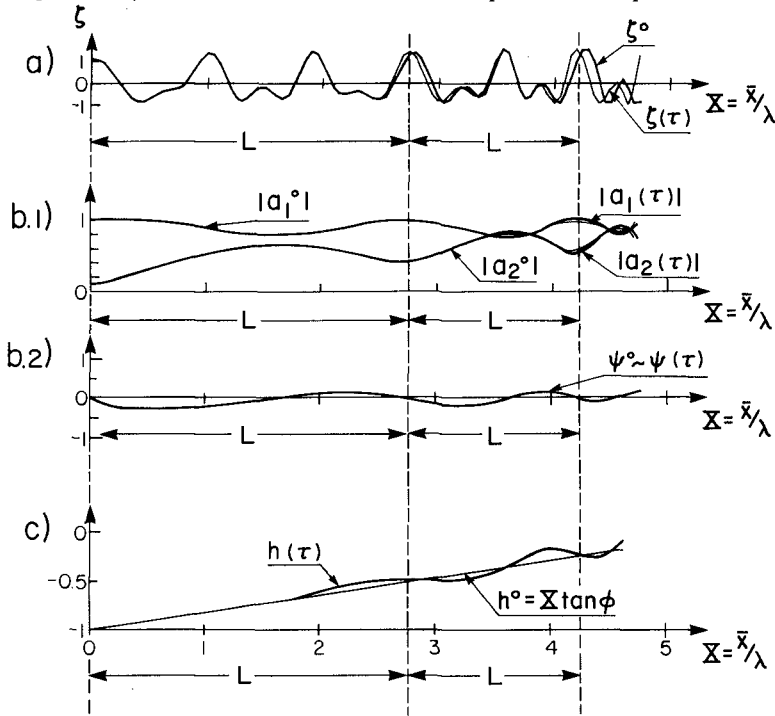


Figure 3. Model predictions of bar formation by cyclonic waves ($T = 17$ s): a) the surface wave profile ζ° , (over h°) and $\zeta(\tau)$ (over $h(\tau)$); b) the Fourier decomposition of ζ into two modal components; c) the initial state h° , and final state $h(\tau)$ of the seabed. The symbol L denotes the repetition length.

The most important aspect of the evolution of the surface wave, which is seen transparently in the evolution of the free surface ζ , is the slow oscillation of the first and second harmonics that is superimposed upon the mean increase in the energy of the second harmonic due to shoaling.

According to the model, energy is exchanged between the modal wave components in a nearly periodic fashion. The horizontal distance between two successive minima of the second harmonic amplitude $|a_2|$ is referred to as the local repetition length L . Such an energy transfer towards higher harmonics has been observed in both laboratory experiments with regular waves (Boczar-Karakiewicz *et al.* 1987) and in spectra of wind waves propagating in a nearshore (Boczar-Karakiewicz and Davidson-Arnott 1987). The repetition length L , which is typically several times the length associated to the surface wave, is also a characteristic length scale in the pattern of the associated velocity field and, consequently, the same scale is induced in the sediment flux pattern Q . The continuity described by equation (6) relates the divergence of the spatially oscillating sediment flux Q , with instantaneous, temporal changes in the bed configuration $h(X)$. Thus, the repetition length L determines the spacing of the sand bars that evolve from the initially featureless bed topography as shown in Figure 3d, (erosion occurs, forming the troughs of the sand bars where $\delta Q/\delta X$ is negative, while sand bar crests are formed where $\delta Q/\delta X$ is positive).

Dynamic equilibrium in a beach system : predictions and comparisons

Formation of sand bars by cyclonic waves simulated on the model and presented in Figure 3 indicate that pronounced changes in the bathymetry may be considered in a zone confined between the isobath of -10 m up to the shoreline. The following experiments are restricted to this narrower part of the nearshore and attention will be focused on time scales of the wave-bed interaction process. Results presented in Figure 3 show two very different time scales considered in the model : the time scale of the surface wave parametrized by its wave period T , and the time scale of bed evolution τ introduced in equation (6). The later can be made explicit by using the parameters of incident waves,

$$\tau = \alpha^5 \beta^{-2} \frac{\bar{f}}{T} \quad (7)$$

and by assuming that sediment concentration and the boundary layer thickness both depend upon the wave amplitude (Boczar-Karakiewicz and Bona 1986). In the following we will investigate the time scale τ carrying out a series of numerical experiments simulating a sequence of wave-bed interaction events typical for the Gold Coast beach system.

The first experiment (Figure 4a) reproduces the event of extreme cyclonic waves ($T = 17$ s, $\alpha = 0.2$; $\beta = 0.5$) resulting in the formation of a two-bar system h . The experiment is initialized now at the water depth of $H = 10$ m from an initial state $h' = X \tan \phi$. The final state h is established after a time $t = 6 \Delta\tau$ (where $\Delta\tau$ denotes the time step

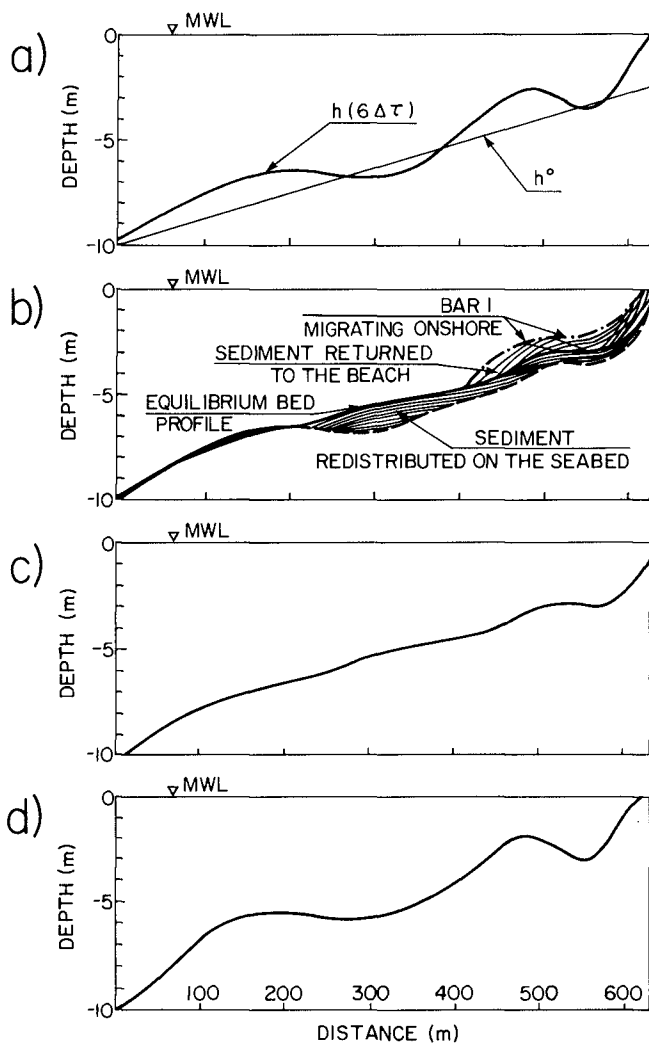


Figure 4. Model predictions of a full cycle of beach transformation: a) formation of a two-bar profile by cyclonic waves ($T = 17$ s) from an initial uniform slope h° ; b) stages of formation of the equilibrium profile by moderate storm waves ($T = 10$ s); c) final equilibrium state; d) reformation of bars by cyclonic waves ($T = 17$ s) from equilibrium state shown in c.

in the present experiment). The second numerical experiment (Figure 4b) simulates moderate storm wave activity ($T = 10$ s, $\alpha = 0.1$, $\beta = 0.1$) which interacts with the seabed which initial state h' that has been formed by cyclonic waves in the previous experiment. Broken lines in Figure 4b represent consecutive stages of the seabed evolution into its final state h of dynamical equilibrium which has been reached after a time $t = 12 \Delta\tau$, (where $\Delta\tau$ denotes the time step in experiment 4b). In the equilibrium state, the seabed remains constant under the action of a wave train of constant parameters. In this state, the offshore bar (bar 1 in Figure 4) is flattened; the trough between bar 1 and bar 2 is filled up with sediment and bar 2 is shifted shorewards. The area between the initial post-cyclonic bed profile and the final equilibrium profile in Figure 4b provides an estimate of sediment volume redistributed on the seabed and of the volume moved onshore, toward the beach. Figure 4c shows again the state of beach equilibrium which constitutes the initial state h' for a following simulation of a cyclonic event under extreme waves ($T = 17$ s, $\alpha = 0.2$, $\beta = 0.05$) presented in Figure 4c. After a time $t = 6 \Delta\tau$, a final state of two bars, denoted by h , is reestablished. Comparisons of h in Figure 4d and 5a shows a close similarity. The final state in Figure 4d terminates a full cycle of nearshore transformation simulated by the sequence of experiments shown in Figure 4b-4d.

The cycle of beach transformation is shown in a three-dimensional version in Figure 5. The initial bar formation (Figure 5a) is followed by two successive stages of profile recovery (Figure 5b) which are terminated by the equilibrium stage (Figure 5c). The stability of the equilibrium state is shown in Figure 5d under moderate storm waves ($T = \text{const}$, $a = \text{const}$). Eventually the reformation of the two-bar post-cyclonic bed profile is shown in Figure 5e.

Time scales in Figures 4 and 5 will now be calibrated using equation (7) and observations from the Gold Coast nearshore. Observations report a typical period of beach recovery under moderate storm conditions in a period of 18 months (Jackson, Smith and Piggot 1988) that provides an estimate of the time step $\Delta\tau$, in the corresponding numerical experiment (Figure 4b), $\Delta\tau = 45$ days. Given the ratio of α and β^{-1} for cyclonic and moderate waves being of the order of 2, the estimate for the time step $\Delta\tau$ in experiment 4a and 4b equals $\Delta\tau = 0.35$ day. Consequently, the period of cyclonic activity forming the two-bar system (Figure 4a and 4d) is approximately equal to two days. Comparisons of model predictions in which the earlier calibrated time scales were used are presented for two sites in the Gold Coast area in Figures 6 and 7. The location of bar crests, their number and dynamics under both extreme and moderate waves is in a quite satisfactory agreement with observations. However, the amplitude of the predicted offshore bar (bar 1) is generally lower than indicated by observations. The latter is maybe not surprising given the extreme simplicity of the model and the extreme complexity of the prototype nearshore.

The post-cyclone seabed profile for the southern part of the Gold Coast area (Kirra, see Figure 1 for location) is presented in Figure 8b. Predictions show that in case of a gradually decreasing mean slope gradient given by observations (Figure 8a) the mean position of the shoreline shifts into the shoreward direction. It may be inferred that

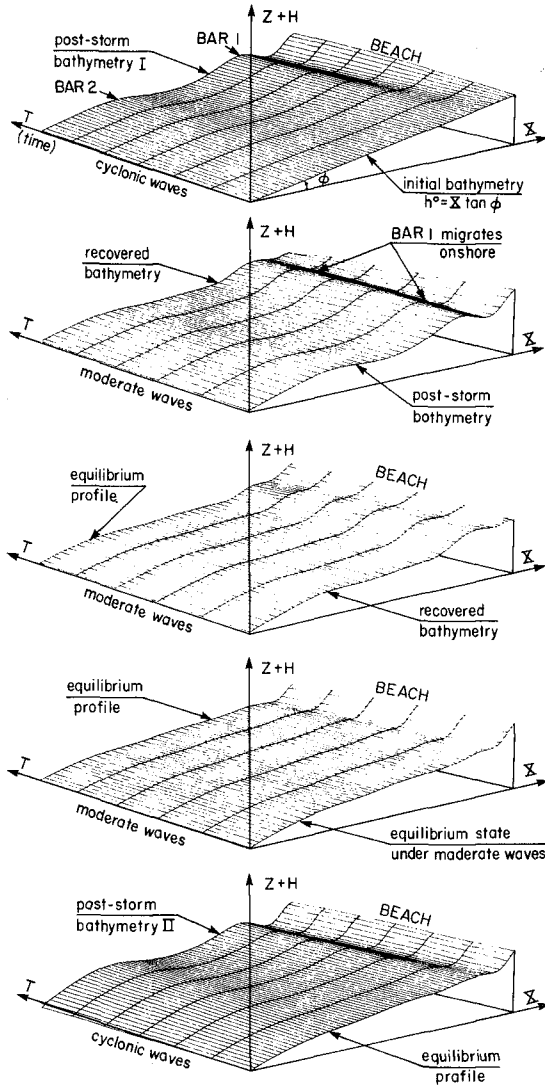


Figure 5. A three-dimensional presentation of model predictions of the cycle of beach transformation : a) formation of post-storm bathymetry by cyclonic waves ($T = 17$ s); b) beach recovery by moderate waves ($T = 10$ s); c) formation of equilibrium by moderate waves ($T = 10$ s); d) equilibrium state under moderate waves ($T = 10$ s); e) bar reformation by cyclonic waves ($t = 17$ s).

observed changes in the nearshore topography are at least partially caused by the deficit of sediment supply in this location, subsequent of the extension of the Tweed River training walls.

3. Conclusions and protection measures for the Gold Coast beach system

The wave-bed interaction model applied in the present paper simulates correctly a typical observed cycle of beach erosion and recovery in the Gold Coast nearshore caused by extreme cyclonic events and followed by periods of moderate storm activity (Figures 4 and 5). Predictions and observations show that beach erosion occurs during a couple of days of an extreme cyclonic event (see Figures 4a and 4d, Figures 5a and 5e) in association with a formation of a prominent two-bar system in the area of the nearshore, limited approximately by a water depth of 10 m. Beach recovery and formation of a nearly uniform featureless equilibrium bed profile has been shown to result from moderate storm wave activity (see Figures 4b-c, Figures 5b-d) during a period of several months.

The simulation of a transformation cycle from post-cyclonic bars into an equilibrium bed profile provides an estimate of sediment volume redistributed over the nearshore and returned to the beach (Figure 4b).

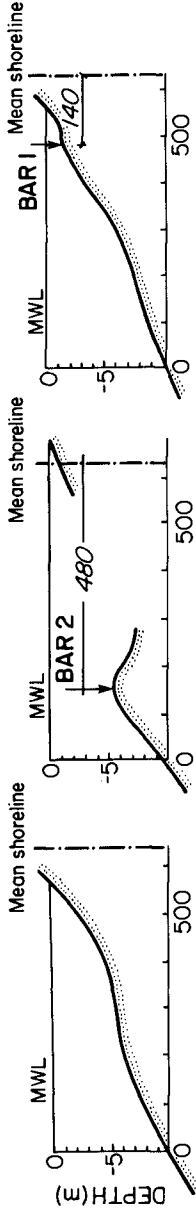
The transformation of the post-cyclonic barred nearshore into recovered equilibrium is shown to be reached when assuming a non-deficit sediment supply and a fully dissipative beach system. The latter requires a conservation of a buffer zone which temporary allows erosion during extreme weather events. The presented beach transformation cycle requires a sufficiently long period of moderate storm-wave activity between two successive extreme storm events (of the order of 18 months, see Figure 5b-c).

In presented calculations, extreme cyclonic waves (characterized by peak periods of 17 secs) were simulated by a regular wave train with a period $t = 17$ s, and a wave amplitude of $a = 2$ m at the incident water depth $H = 19$ m. Moderate wave activity was simulated with an incident wave train of a wave period $T = 10$ s and an amplitude $a = 1.0$ m at the incident water depth $H = 10$ m. Model predictions compared with observations in two chosen locations of the central Gold Coast area have shown a satisfactory agreement for both the pre- and post-cyclonic bars (see Figures 6 and 7).

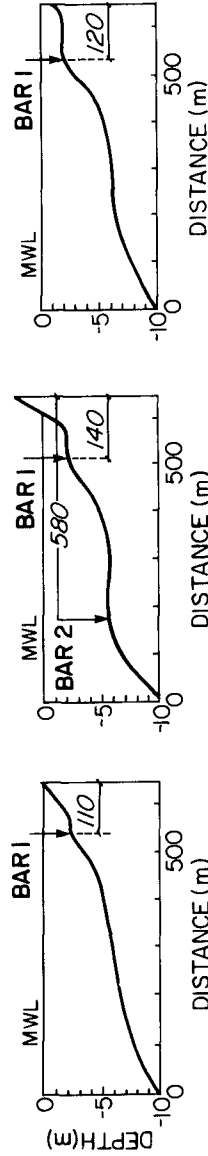
Presented results compared with available observations suggest beach protection measures in the Gold Coast area, which would compensate progressing erosion resulting from a deficit in sediment supply and from development pressures.

Suggested method of beach nourishment consists of the formation of a post-cyclonic profile, i.e. in placing sediment pumped from offshore in the location of the two offshore bars. The volume of the placed sediment will compensate the local deficit in the sediment supply, will be partially redistributed over the active nearshore and be partially returned to the beach after several months of moderate wave activity. The reconstruction of bars by beach nourishment will additionally provide protection to the beach due to energy dissipation caused by a multiple offshore breaking of the incident wave. However, according to presented results, sediment for nourishing the nearshore

[i] MEASURED BATHYMETRIES (1967-68)



[ii] MODEL PREDICTIONS



a) PRE-STORM PROFILES b) POST-STORM PROFILES c) RECOVERED PROFILES

Figure 6. Comparison of measured and predicted bathymetries at Surfers Paradise for a) pre-storm conditions; b) post-storm conditions; and for c) beach recovery.

PRE-STORM

POST-STORM

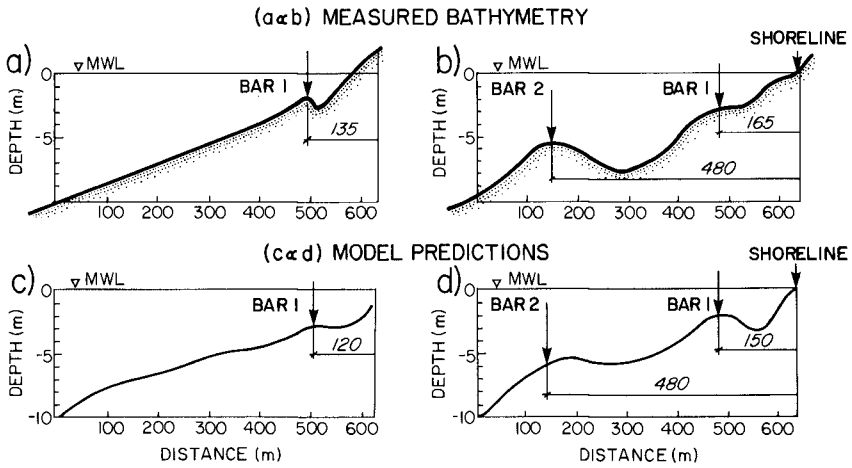


Figure 7. Comparison of model predictions with measured bathymetries : pre- and post-storm bathymetries at Broadbeach.

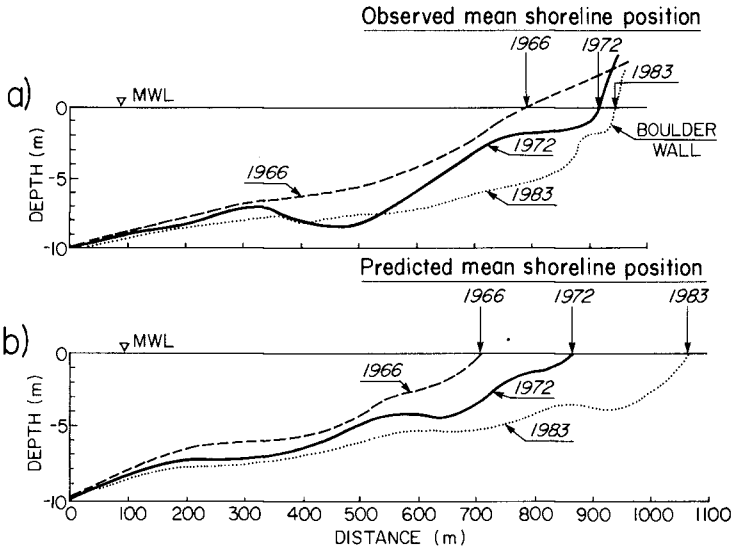


Figure 8. Observed (a) and predicted (b) shoreline recession due to changes in the mean slope of the underwater beach at Kirra.

should be removed from areas lying deeper than the isobath -20 m which constitutes the outer limit of the active nearshore for extreme cyclonic waves.

Results of model simulation in the area of Kirra (Figure 8) indicate that construction of seawalls is only a temporary measure of protection. The constantly decreasing mean nearshore slope of the seabed in this region due to acute sediment deficit results in a constant shoreward shift of the mean shoreline position. The latter causes slumping of seawalls which themselves have a negative effect on nearshore stability associated with strong wave reflection.

Acknowledgements

Support for this project was provided by the Ministry of Fisheries and Oceans (Government of Canada) and by the Natural Sciences and Engineering Research Council of Canada (Grant no A2621). Both authors also acknowledge the Gold Coast City Council, QLD, Australia, for releasing survey data for this publication.

References

- Boczar-Karakiewicz, B. and J.L. Bona. 1986. Scale effects in modelling sand bar formation in coastal regions by progressive surface waves. Symposium '86. Int. Ass. Hydr. Res. (IAHR), Toronto, Proceedings : 49-61 (ed. A.S. Yalin).
- Boczar-Karakiewicz, B., J.L. Bona and D.L. Cohen. 1987. Interaction of shallow-water waves and bottom topography. *In* : Dyn. Problems Cont. Physics, Springer-Verlag, 4 : 131-175.
- Boczar-Karakiweicz, B. and R.D.L. Davidson-Arnott. 1987. Nearshore bar formation by non-linear wave processes - A comparison of model results and field data. *Mar. Geol.*, 77 : 287-304.
- Boczar-Karakiewicz, B., A. Létourneau, Y. Gratton and B. Pelchat. 1990. Oblique incident waves in a shore-parallel bar system. *Can. Coastal Conf.*, Kingston, (ed. M. Davies). : Proceedings : 99-109.
- Chapalain, G. and B. Boczar-Karakiewicz. 1989. Longshore bar formation in coastal wave-dominated areas. XXIII Congress of Int. Ass. Hydr. Res., Ottawa, Proc., Tech. Session C : C531-C538.
- Chapman, D.M. 1980. Beach nourishment as a management technique. Proc. 17th Int. Coast. Eng. Conf., Sydney : 86-92.
- Gold Coast City Council, 1990, Coastal Engineering Works, Internal Report
- Jackson, L.A., A.W. Smith and T. Piggot. 1988. Data for coastal management in a beach zone. *Coast. Zone Manag.* 88 Workshop, Lismore. Proceedings : 102-110.
- McGrath, B.L. and D.C. Patterson. 1972. Wave climate at Gold Coast, Qld, Australia. *Inst. Eng. Aust.*, 8 Div. Tech. Papers 13 (5) : 1-17.
- Smith, A.W. and L.A. Jackson. 1990. The siting of beach nourishment placements. *Shore and Beach*, 58 (1) : 17-24.